Developing Power-Law Fluid Flow in The Entrance Region of a Parallel Plate Channel

DEVELOPING POWER-LAW FLUID FLOW IN THE ENTRANCE REGION OF A PARALLEL PLATE CHANNEL

by

Sadia Rehman

A Thesis presented to the faculty of the
American University of Sharjah
College of Engineering
In Partial Fulfilment
of the Requirements
for the Degree of

Master of Science in
Chemical Engineering

Sharjah, United Arab Emirates

(March 2024)

Declaration of Authorship

I declare that this project/thesis/dissertation is my own work and, to the best of my knowledge and belief, it does not contain material published or written by a third party, except where permission has been obtained and/or appropriately cited through full and accurate referencing.

Signed…………………… Sadia Rehman……………………………

Date……………………….22/04/24…………………………………

Approvals

We, the undersigned, approve the Master's Thesis written by: Sadia Rehman

Thesis Title: Developing Power-Law Fluid Flow in The Entrance Region of a Parallel Plate Channel.

Date of Defense: 22/04/24

Name, Title and Affiliation	**Signature**
Dr. Rachid Chebbi Professor, Department of Chemical and Biological Engineering Thesis Advisor	
Dr. Zarook Shareefdeen Professor, Department of Chemical and Biological Engineering Thesis Committee Member	
Dr. Mehmet Orhan Associate Professor, Department of Mechanical Engineering Thesis Committee Member	

Accepted by:

Dr. Fadi Aloul
Dean
College/School of Engineering

Dr. Mohamed El-Tarhuni
Vice Provost for Research and Graduate Studies
Office of Research and Graduate Studies

Acknowledgements

I express my deepest gratitude to God for his help and guidance, without which I would not be able to manage the complexities of research and academia. I want to thank my advisor Dr Rachid Chebbi for being extremely supportive, understanding and guiding me throughout my research journey. I'm deeply indebted for his ongoing mentoring, advice and valuable assistance.

With gratitude, I extend my heartfelt appreciation to my thesis committee members: Dr Zarook Sharefdeen and Dr Mehmet Orhan. Their feedback aided me in elevating the quality of my work. I also extend my sincere appreciation to the American University of Sharjah for providing me with the opportunity to complete my graduate study and provide me with a Graduate Teaching Assistantship which has been crucial for my academic endeavours.

I am profoundly grateful to my family, particularly my parents for their constant support throughout my master's journey.

Dedication

To my family and friends…

Abstract

Non-Newtonian fluids are used in different processes including heat exchangers, extrusion processes and chemical production. Numerous significant industrial fluids exhibit non-Newtonian properties. Many non-Newtonian fluids are modelled as power-law fluids. Research on the laminar flow of power-law fluids in the entrance region of parallel plates has been conducted by previous investigators using a variety of methods. The main objective of this research is to model power-law fluid flow in the entrance region of parallel plate channels using the inlet-filled region concept. The problem is solved using a modified boundary layer integral method and the results are validated against published data. The results for the inlet and filled regions include velocity, pressure drop and boundary layer thickness profiles in addition to the inlet and filled region sizes as functions of the power-law index. The present model results asymptotically reach the fully developed velocity profile, friction factor and centreline velocity values for power-law fluids and demonstrate strong consistency with published Newtonian fluid flow results in the entrance region of parallel plates.

Keywords: Power-law; Non-Newtonian; Laminar Flow; Hydrodynamic Entrance Region; Von Kármán Momentum Integral Method, Inlet Region, Filled Region.

Table of Contents

List of Figures

List of Abbreviation

English Letters

C_f	Local friction factor
K	Consistency index
n	Power-law fluid index
P	Pressure
P_O	Inlet pressure
q	$1+1/n$
Re	Reynolds number
U_o	Uniform velocity
u	Velocity component in the x-direction
U_c	Centerline velocity
$\bar{U}_\infty$	Dimensionless velocity in the core region
$\bar{U}_c$	Dimensionless centerline velocity
v	Velocity component in the y-direction
x	Axial distance
y	Distance from the wall

Greek Letters

η	Apparent viscosity
δ	Boundary layer thickness
ρ	Fluid density
τ	Shear stress
τ_w	Shear wall stress
α	Dimensionless Slope of the velocity profile
λ	Pressure gradient parameter
Γ	Shape Factor
ζ	Dimensionless coordinate
ξ	Dimensionless axial distance
δ_{1i}, δ_{2i}	Displacement thickness and Momentum thickness in the inlet region
δ_{1f}, δ_{2f}	Displacement thickness and Momentum thickness in the filled region
$\bar{\delta}_{1i}, \bar{\delta}_{2i}$	Dimensionless displacement and Momentum thickness in the inlet region
$\bar{\delta}_{1f}, \bar{\delta}_{2f}$	Dimensionless displacement and Momentum thickness in the filled region
$\Delta\bar{P}$	Dimensionless pressure drop

Chapter 1. Introduction

1.1. Non-Newtonian Fluids

Chemical solutions and mixtures of solid particles and liquids are used in a variety of engineering operations on geological formations, such as improved hydrocarbon recovery, soil remediation, and drilling operations. Industrial and environmental applications can benefit from a clear understanding of complex fluid flows by lowering costs, minimizing impact, and fostering cutting-edge design optimization methods [1]. The flow and heat transfer in the entrance region have been a topic of interest from both a practical and theoretical point of view. In recent years, several studies have been conducted on the applications of fluid flow between parallel plates such as microfluidics [2], food processing [3] and blood flow in microchannels [4]. The behaviour of fluids is initially categorized as either Newtonian, Non-Newtonian or Viscoelastic. The fluids in many petrochemical, food and pharmaceutical industries are often non-Newtonian.

Non-Newtonian fluids are further classified into time-dependent and time-independent. Time-independent fluids are those whose rheological behavior (at constant temperature) depends solely on the shear stress. Time-independent fluids may further be grouped as pseudoplastic (shear thinning), Bingham plastic (shear thinning), and dilatant (shear-thickening). On the other hand, time-dependent fluids are divided into Thixotropic fluids and Rheopectic fluids. Viscoelastic fluids are defined as fluids that exhibit both viscous and elastic properties.

1.2. Overview

Many non-Newtonian fluids are pseudoplastic. The power law model [5] (Ostwald–de Waele relationship), the relationship between the shear stress and the shear rate is given by:

$$\tau = K(dv/dy)^{n} \tag{1}$$

$$\eta = K(dv/dy)^{(n-1)} \tag{2}$$

When referring to Newtonian fluids, K is typically represented by the symbol μ, which is the fluid viscosity, with the flow behavior index n being set to 1.

Pseudoplastic (n<1) fluids exhibit a thinning behaviour at high shear rates because their apparent viscosity decreases with increasing shear rate and Dilatant fluids (n>1) are shear thickening. Several substances act as pseudoplastic fluids, including polymer solutions, lubricants, rayon synthesis, detergent slurries, and cellulose derivatives and their solutions. Pseudoplastic fluids do not thicken at high shear rates, but dilatant fluids do [5].

In the present model, the entrance region is divided into two zones using the inlet-filled region concept introduced by Ishizawa [6]: in the inlet region, viscous effects are restricted to the boundary layer, and in the filled region, the flow is developing with viscous effects present in any part of that region. The area, where viscous effects are present develops, increases and significantly grows is known as the boundary layer. In the core region, potential flow exists with viscous effects essentially non-existent. The boundary layer grows and ultimately encloses the cross-sectional region at some point along the direction of the axis. According to Ishizawa [6] and Mohanty and Asthana [7], this point denotes the end of the inlet region but not the entrance region, indicating that the velocity profile has not yet been fully developed.

The flow of the fluid is considered to be laminar with relevant physical properties assumed to be constants. The main objective of this research is to solve the hydrodynamic entry length problem using the inlet-filled region concept with a modified von Karman momentum integral method. This is done for a power-law fluid flowing through a parallel plate to solve the continuity and momentum equations. The expected results for the inlet and filled regions include the velocity, pressure and boundary layer thickness profiles and the inlet and filled region as a function of the generalized Reynolds number.

1.3. Thesis Objectives

The primary objective of the thesis is to apply the inlet-filled region concept to power-law fluid flow in a parallel plate channel using a momentum integral method to solve for developing fluid flow in the channel.

1.4. Research Contribution

This thesis solves the entrance region problem of a parallel plate channel for a power-law fluid flow fluid. This includes the velocity, pressure drop and local friction factor profiles. The results for the inlet and filled regions include the velocity, pressure and boundary layer thickness profiles and the inlet and filled region as a function of the generalized Reynolds number. The results asymptotically match the fully developed profiles and are in better agreement with the accurate Newtonian fluid finite difference solution in [16] as compared to other published results. In addition, the method is predominantly analytical.

1.5. Thesis Organization

The rest of the thesis is organized as follows: Chapter 2 provides background about the inlet-filled concept and its importance. Moreover, related works to this research are discussed and the merits of the inlet-filled concept are discussed. The governing equations for flow in the inlet and filled regions are discussed in Chapter 3. Chapter 4 presents and analyses the results obtained. Chapter 5 concludes the thesis and suggests extensions to the present investigation.

Chapter 2. Background and Literature Review

Many researchers have investigated the length of the entrance region both analytically and numerically. The traditional boundary-layer technique is discussed.

2.1. The Boundary-layer theory

There were two schools of thought on fluid mechanics in the late nineteenth century. The first group, the hydraulicians, used empirical equations and experimental data. Hydrodynamicists, on the other hand, used the fundamental conservation principles. The hydrodynamicists proposed a perfect fluid with zero viscosity and constant density since the associated differential equations were typically too complex to solve [8]. They failed to solve flow problems in channels and pipes, but their mathematical solutions matched quite well for flows that did not include solid surfaces, such as tides. Ludwig Prandtl introduced the boundary layer concept in 1904. He suggested conceptually splitting the flow region into two sections. A region near the solid surface where, the viscous effects there are too large to be disregarded and the remaining region in which viscous effects can be disregarded and where the rules of perfect-fluid flow can be used.

Prandtl began with the distinct understanding that the behaviour of the fluid at the wall of the solid barrier is the most crucial issue pertaining to the flow of a fluid past a wall. Very close to the wall, it appears that the flow is almost irrotational. Hence the change in velocity from the value associated with irrotational motion to the zero-velocity required by the condition of no slip at the wall occurs within a tiny layer next to the wall. The transition layer becomes thinner as the viscosity decreases. Nonetheless, the high-velocity slope generates noticeable effects that are comparable in size to those caused by the inertia force despite the low viscosity, when the thickness of the transition layer is proportional to the square root of the kinematic viscosity [9]. As a result, the boundary layer is a thin transition layer where viscosity effects are most noticeable. Outside of this layer, the flow is essentially viscosity-free and accurately represented by an irrotational motion.

2.2. Earlier Work Done

Schiller [10] was one of the early researchers to apply an integral method to a Newtonian fluid model with a developing boundary layer and an inviscid core in the flow of a pipe. In this approach, the velocity profile is in the form of a polynomial. He assumed a velocity distribution that is parabolic in shape inside the boundary layer. To this, a mechanical energy balance was applied exclusively to the inviscid core. This resulted in the neglection of the viscous dissipation in the boundary layer. Several assumptions were made by various researchers such as Langhaar [11] applied the linearization approach to the differential momentum balance to obtain an approximate solution in circular pipes, Boussinesq [12] solved the approximate solution using a perturbation term far from the entrance of the tube, Atkinson and Goldstein [13] modified Boussinesq’s approach by employing stream function to find the solution. Seigel [14] extended Schiller’s work by applying it as cubic and quartic velocity representation. Following this, Campbell and Slattery [15] utilized the same parabolic profile used by Schiller while including the viscous dissipation in the boundary layer.

Bodoia and Osterle [16] utilized the finite-difference method in solving the two-dimensional fluid flow in channels using a boundary layer model. Their results included the determination of the variations of pressure and velocity. In addition, they determined the relationship between the entrance region size and Reynolds number.

Yau and Tien [17] employed the mass and momentum integral approach using an alternate fourth-order polynomial velocity profile at the entrance region of the power-law fluid in flat ducts. The entrance region considered is limited to the point where the boundary layer thickness reaches half the space between the two plates. Entrance length, dimensionless boundary layer, velocity profile and pressure drop are provided for different values of the power-law index. In addition to this, the approximate velocity profile calculated by Yau and Tien [17] does not exactly match the analytically estimated fully developed velocity profile at x equal to the hydrodynamic length.

Magno et al. [18] applied the generalized integral transform method used in the parallel plate channel laminar flow of power-law non-Newtonian fluids while solving the boundary layer equations numerically. This method uses the stream function instead of the primary variables (pressure and velocity).

Crespí-Llorens and Galanis [19] extended the analysis of Campbell and Slattery [15] from the case of Newtonian fluid flow in a tube to the case of power-law fluid between parallel plates. The approximate velocity profile in the inlet region is selected such that it matches the well-known velocity profile in the fully developed flow. The entrance region is restricted to the boundary layer zone, referred to as the inlet region. Crespí-Llorens and Galanis noted that the velocity profile selected by Yau and Tien[17] does not exactly match the analytically estimated fully developed velocity profile at the end of the boundary layer zone.

Lambride et al. [20] solved for the primary variables numerically using the finite element method. The results yield the length of the entrance region using the centerline velocity and local friction factor criteria.

In most studies, including the fluid flow of Newtonian fluids, the flow in the entrance region is considered to consist of one zone in which the boundary layer thickness increases till viscous effects cover the whole area of the flow. However, this assumption was discarded by Goldstein [21] and Rosenhead [22] as it produced incoherence in the slope of the velocity profile at the end of the entrance region. Ishizawa [6] introduced the inlet-filled region concept by including a filled region in which viscous effects in the whole cross-sectional area are present with the velocity profile asymptotically reaching the fully developed profile.

Ishizawa's concept applied to radial flow between parallel disks [6] was extended by Mohanty and Asthana [7] and Mohanty and Das [23] to investigate the developing flow in the entrance region for both a circular tube and a parallel plate channel respectively.

Al-Ali and Selim [24] extended the inlet-filled region concept to the case of simultaneously developing fluid through a parallel plate channel with constant heat flux and heat transfer. After the successful extensions of Ishizawa's inlet-filled region concept [6] applied to Newtonian fluids in [7,22,23], Chebbi [25] extended the same concept to power-law fluid flow in a circular pipe and led to results for the entry length size as a function of the generalized Reynolds number, the boundary layer thickness, velocity profile, pressure drop and local friction factor. The same concept was extended by Baioumy et al. [26] to developing Bingham fluid flow for the same circular pipe geometry with the results being successful. We extend the inlet-filled region concept to investigate developing flow in a parallel plate channel.

In our investigation, we present a new analytical solution for the entry length problem for power-law fluid flow in a parallel plate channel.

Chapter 3. Methodology

3.1. Governing Equations

Consider the continuous laminar flow that occurs when an incompressible fluid enters at a uniform velocity at the inlet. Figure 3-1 shows the physical model for the entrance region of a parallel plate channel.

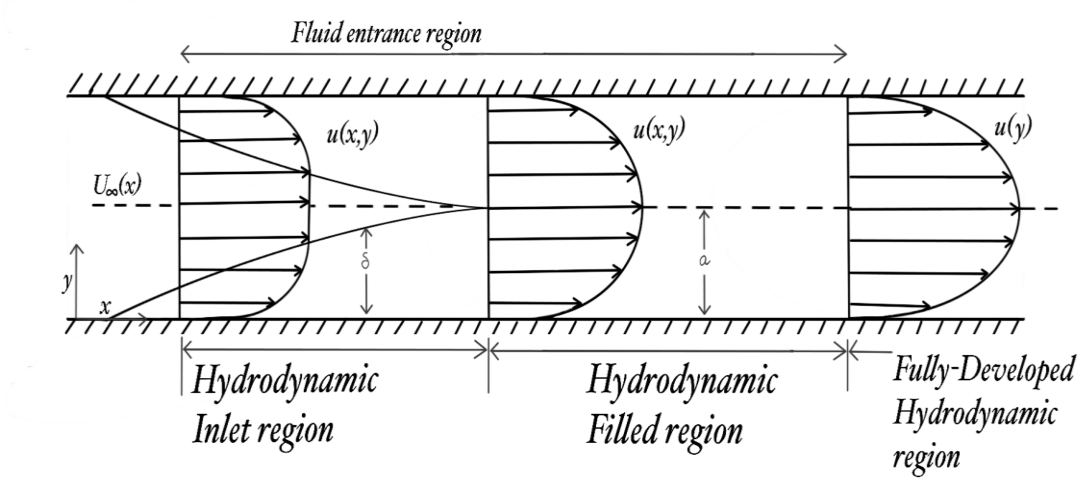

Figure 3-1: Physical model and coordinate system for the flow in the entrance region of a parallel plate channel.

We assume steady state conditions. Viscous dissipation effects are neglected, and physical properties are considered constant.

The governing equations include conservation of mass and momentum equations using a boundary layer model.

Continuity Equation:

$$\frac{\partial u}{\partial x}+\frac{\partial v}{\partial y}=0 \tag{3}$$

Momentum Equations:

$$u\frac{\partial u}{\partial x}+v\frac{\partial u}{\partial y}=\frac{K}{\rho}\frac{\partial}{\partial y}\left[\left(\frac{\partial u}{\partial y}\right)^{n}\right]-\frac{1}{\rho}\frac{\partial P}{\partial x} \tag{4}$$

$$\frac{\partial P}{\partial y}=0 \tag{5}$$

where u and v represents the velocity components in the x and y directions respectively and P denotes pressure.

Using Ishizawa's [6] inlet-filled concept, the entrance region is divided into two regions namely, inlet and filled region.

3.2. Inlet Region

This is the region where viscous effects are limited to the boundary layer. In the core region, viscous effects are neglected. This leads to:

Core region:

$$U_\infty \frac{dU_\infty}{dx} = -\frac{1}{\rho}\frac{\partial P}{\partial x} \tag{6}$$

Substituting Equation (4) in Equation (2)

Boundary layer region:

$$u\frac{\partial u}{\partial x} + v\frac{\partial u}{\partial y} = \frac{K}{\rho}\frac{\partial}{\partial y}\left[\left(\frac{\partial u}{\partial y}\right)^n\right] + U_\infty \frac{dU_\infty}{dx} \tag{7}$$

where, u and v are velocity components in the x and y directions, respectively, ρ is density, U_∞ is the velocity in the core and P is the pressure.

The inlet region boundary conditions are:

$$u = U_O \qquad at\ x = 0 \tag{8}$$

$$P = P_O \qquad at\ x = 0 \tag{9}$$

$$u = 0\ ;\ v = 0 \qquad at\ y = 0 \tag{10}$$

$$u = U_\infty\ (x) \qquad at\ y = \delta(x) \tag{11}$$

$$\frac{\partial u}{\partial y} = 0 \qquad at\ y = \delta(x) \tag{12}$$

Following Chebbi [25], we define $\alpha\ and\ \lambda$ in the inlet region as,

$$\alpha = \frac{\delta}{U_\infty}\left(\frac{du}{dy}\right)_{y=0} \tag{13}$$

$$\lambda = \frac{\rho}{K}\frac{\delta^{n+1}}{\alpha^{n-1}}\frac{1}{U_\infty^{n-1}}\frac{dU_\infty}{dx} \tag{14}$$

Using the equation of continuity gives

$$\frac{\partial u}{\partial x} = -\frac{\partial v}{\partial y} \tag{15}$$

Therefore,

$$u\frac{\partial u}{\partial x} = \frac{\partial u^2}{\partial x} - u\frac{\partial u}{\partial x} \tag{16}$$

Applying the equation of continuity, we get

$$u\frac{\partial u}{\partial x} = \frac{\partial u^2}{\partial x} + u\frac{\partial v}{\partial x} \tag{17}$$

Substituting equation (17), in the boundary layer equation (7) gives

$$\frac{\partial u^2}{\partial x} + u\frac{\partial v}{\partial x} + v\frac{\partial u}{\partial y} = \frac{K}{\rho}\frac{\partial}{\partial y}\left[\left(\frac{\partial u}{\partial y}\right)^n\right] + U_\infty\frac{dU_\infty}{dx} \tag{18}$$

Integrating the above equation from $y = 0$ to $y = \delta(x)$ yields:

$$\int_0^\delta \frac{\partial u^2}{\partial x}dy + \int_0^\delta \frac{\partial(uv)}{\partial y}dy = \int_0^\delta \frac{K}{\rho}\frac{\partial}{\partial y}\left[\left(\frac{\partial u}{\partial y}\right)^n\right]dy + \int_0^\delta U_\infty\frac{dU_\infty}{dx}dy \tag{19}$$

Applying the boundary conditions, we obtain:

$$\int_0^\delta \frac{\partial u^2}{\partial x}dy + U_\infty v_{y=\delta} = \frac{K}{\rho}\left[\left(\frac{\partial u}{\partial y}\right)^n\right] + \frac{dU_\infty}{dx}\int_0^\delta U_\infty\, dy \tag{20}$$

Integrating the continuity equation from $y = 0$ to $y = \delta(x)$ gives:

$$v_{y=\delta} = -\int_0^\delta \frac{\partial u}{\partial x}dy \tag{21}$$

Substituting $v_{y=\delta}$ in the previous equation, we get

$$\int_0^\delta \frac{\partial u^2}{\partial x}dy - U_\infty\int_0^\delta \frac{\partial u}{\partial x}dy = \frac{K}{\rho}\left[\left(\frac{\partial u}{\partial y}\right)^n\right]_{y=0} + \frac{dU_\infty}{dx}\int_0^\delta U_\infty\, dy \tag{22}$$

Using the Leibnitz's rule in the above equation, the two sections of the left-hand side can be expressed as follows:

$$\int_0^\delta \frac{\partial u^2}{\partial x}dy = \frac{d}{dx}\int_0^\delta u^2\, dy - U_\infty^2\frac{d\delta}{dx} \tag{23}$$

$$U_\infty \int_0^\delta \frac{\partial u}{\partial x} dy = \frac{d}{dx}\int_0^\delta u U_\infty\, dy - \frac{dU_\infty}{dx}\int_0^\delta u\, dy - U_\infty^2 \frac{d\delta}{dx} \tag{24}$$

Substituting the above two equations in the left-hand side of equation (22):

$$\begin{aligned} &\frac{d}{dx}\int_0^\delta u^2\, dy - U_\infty^2 \frac{d\delta}{dx} - \frac{d}{dx}\int_0^\delta u U_\infty\, dy + \frac{dU_\infty}{dx}\int_0^\delta u\, dy + U_\infty^2 \frac{d\delta}{dx} \\ &= \frac{K}{\rho}\left[\left(\frac{\partial u}{\partial y}\right)^n\right]_{y=0} + \frac{dU_\infty}{dx}\int_0^\delta U_\infty\, dy \end{aligned} \tag{25}$$

Thus, the following is obtained:

$$\frac{d}{dx} U_\infty^2 \int_0^\delta \left[1 - \frac{u}{U_\infty}\right]\frac{u}{U_\infty} dy + \frac{dU_\infty}{dx} U_\infty \int_0^\delta \left[1 - \frac{u}{U_\infty}\right] dy = \frac{K}{\rho}\left[\left(\frac{\partial u}{\partial y}\right)^n\right]_{y=0} \tag{26}$$

Defining the displacement thickness, δ_{1i} and momentum thickness, δ_{2i} from the above equation:

$$\delta_{2i} = \int_0^\delta \left[1 - \frac{u}{U_\infty}\right]\frac{u}{U_\infty} dy \tag{27}$$

$$\delta_{1i} = \int_0^\delta \left[1 - \frac{u}{U_\infty}\right] dy \tag{28}$$

Substituting the above definitions in the equation, we get:

$$\frac{d}{dx} U_\infty^2 \delta_{2i} + \frac{dU_\infty}{dx} U_\infty \delta_{1i} = \frac{K}{\rho}\left[\left(\frac{\partial u}{\partial y}\right)^n\right]_{y=0} \tag{29}$$

3.2.1. Conservation of mass in the inlet region

The overall mass balance is as followed:

$$\int \rho u dA = \rho U_o A \tag{30}$$

Where A is the cross-sectional area for flow.

Dividing by $2w\rho$ on both sides, where *w* is the width of the channel:

$$aU_o = \int_0^\delta u\, dy + \int_\delta^a U_\infty\, dy \tag{31}$$

Then, dividing by U_∞ on both sides to the above equation:

$$\frac{aU_o}{U_\infty} = \int_0^\delta \frac{u}{U_\infty} dy + \int_\delta^a 1\, dy \tag{32}$$

Integrating with respect to y gives:

$$\frac{aU_o}{U_\infty} = \int_0^\delta \frac{u}{U_\infty} dy + (a - \delta) \tag{33}$$

Adding δ to both sides of equation (33) yields

$$\frac{aU_o}{U_\infty} = -\int_0^\delta \left(1 - \frac{u}{U_\infty}\right) dy + \delta + (a - \delta) \tag{34}$$

Rearranging the above equation gives

$$\int_0^\delta \left(1 - \frac{u}{U_\infty}\right) dy = a\left(1 - \frac{U_o}{U_\infty}\right) \tag{35}$$

The above equation (35) shows that the displacement thickness, δ_{1i} is equal to

$$\delta_{1i} = a\left(1 - \frac{U_o}{U_\infty}\right) \tag{36}$$

Hence, the conservation of mass in the inlet region gives:

$$\frac{U_o}{U_\infty} = 1 - \frac{\delta_{1i}}{a} \tag{37}$$

3.2.2. Dimensionless form in the inlet region

The Reynolds Number, Re for the flow is expressed:

$$Re = \frac{\rho U_o^{2-n}(4a)^n}{K} \tag{38}$$

The dimensionless boundary layer thickness is defined as:

$$\bar{\delta} = \frac{\delta}{a} \tag{39}$$

The dimensionless axial distance is defined in the inlet and filled regions as:

$$\xi = \frac{x}{aRe} \tag{40}$$

The remaining dimensionless variables are defined as follows:

$$\bar{\delta}_{1i} = \frac{\delta_{1i}}{a} \tag{41}$$

$$\bar{\delta}_{2i} = \frac{\delta_{2i}}{a} \tag{42}$$

$$\bar{U}_{\infty} = \frac{U_{\infty}}{U_o} \tag{43}$$

The dimensionless coordinate in the y-direction is defined as:

$$\zeta = 1 - \frac{y}{\delta} \tag{44}$$

The dimensionless equation of the pressure drop is defined as:

$$\Delta\bar{P} = \frac{P_O - P}{\rho U_o^2/2} \tag{45}$$

Integrating equation (6) gives

$$\Delta\bar{P} = \bar{U}_{\infty}^2 - 1 \tag{46}$$

The dimensionless local friction factor, defined as

$$C_f = \frac{\tau_w}{\rho U_o^2/2} \tag{47}$$

where τ_w is the shear stress of the wall, is given by

$$C_f\, Re = 2.\left\lfloor 4^n \alpha^n \bar{U}_{\infty}^n / \bar{\delta}^n \right\rfloor \tag{48}$$

The dimensionless equation of conservation of mass in the inlet region is expressed using equation (37) as:

$$\frac{1}{\bar{U}_{\infty}} = 1 - \bar{\delta}_{1i} \tag{49}$$

The dimensionless equation for equation (29) is expressed as:

$$\frac{d}{d\xi}\left(\bar{U}_{\infty}{}^2\, \bar{\delta}_{1i}\right) + \frac{d\bar{U}_{\infty}}{d\xi}\bar{U}_{\infty}\bar{\delta}_{1i} = \frac{4^n \bar{U}_{\infty}^n}{\bar{\delta}^n}\left(-\frac{\partial u}{\partial \zeta}\right)^n \tag{50}$$

The derivatives of the dimensionless displacement thickness $\bar{\delta}_{1i}$ and the dimensionless momentum thickness $\bar{\delta}_{2i}$ with respect to ξ are given by:

$$\frac{d\bar{\delta}_{1i}}{d\xi} = \frac{\lambda\, 4^n \bar{U}_{\infty}{}^{n-3} \alpha^{n-1}}{\bar{\delta}^{n+1}} \tag{51}$$

$$\frac{d\bar{\delta}_{1i}}{d\xi} = \frac{4^n \bar{U}_\infty{}^{n-2} \alpha^{n-1}}{\bar{\delta}^n} \left[\alpha - \frac{\lambda}{\bar{\delta}} \left(2\bar{\delta}_{2i} + \bar{\delta}_{1i} \right) \right] \tag{52}$$

3.2.3. Solution of the inlet region flow problem

To solve the above equations above, we use the following approximate profile:

$$\bar{u} = (1 + \zeta^q)(a_1 + a_2\zeta + a_3\zeta^2) \tag{53}$$

Using the boundary conditions yields the following equations:

$$(a_1 + a_2 + a_3) = -1 \tag{54}$$

$$a_1 = 0 \tag{55}$$

Similarly, the remaining coefficients of the above velocity profile is shown below:

$$a_2 = -1 + \frac{\lambda}{2n(q+1)} - \frac{q}{2} \tag{56}$$

Substituting equations (55) and (56) into equation (54) yields:

$$a_3 = \frac{q}{2} - \frac{\lambda}{2n(q+1)} \tag{57}$$

Thus, the approximate velocity profile in the inlet region is given by:

$$\bar{u} = (1 + \zeta^q) \left[\left(-1 + \frac{\lambda}{2n(q+1)} - \frac{q}{2} \right) \zeta + \left(\frac{q}{2} - \frac{\lambda}{2n(q+1)} \right) \zeta^2 \right] \tag{58}$$

Using the above velocity profile and integrating equation (28) yields:

$$\bar{\delta}_{1i} = -\bar{\delta} \left(\frac{a_2}{q+2} + \frac{a_3}{q+3} \right) \tag{59}$$

Similarly, the momentum thickness, $\bar{\delta}_{2i}$ is obtained using MATLAB tool for integration:

$$\bar{\delta}_{2i} = -\bar{\delta} \left(\frac{a_2^2}{2q+3} + \frac{a_3^2}{2q+5} + \frac{a_3}{q+3} + \frac{a_2(a_3+1)}{q+2} \right) \tag{60}$$

Differentiating the dimensionless displacement $\bar{\delta}_{1i}$ and momentum $\bar{\delta}_{2i}$ thickness and using the chain rule yields

$$\frac{d\bar{\delta}}{d\xi} = \frac{\frac{d\bar{\delta}_{1i}}{d\xi} G_{22i} - \frac{d\bar{\delta}_{2i}}{d\xi} G_{12i}}{G_{11i}G_{22i} - G_{21i}G_{12i}} \tag{61}$$

and

$$\frac{d\lambda}{d\xi} = \frac{\frac{d\bar{\delta}_{2i}}{d\xi} G_{11i} - \frac{d\bar{\delta}_{1i}}{d\xi} G_{21i}}{G_{11i}G_{22i} - G_{21i}G_{12i}} \tag{62}$$

where,

$$G_{11i} = \frac{\partial \bar{\delta}_{1i}}{\partial \bar{\delta}}, \qquad G_{12i} = \frac{\partial \bar{\delta}_{1i}}{\partial \lambda}, \qquad G_{21i} = \frac{\partial \bar{\delta}_{2i}}{\partial \bar{\delta}}, \qquad G_{22i} = \frac{\partial \bar{\delta}_{2i}}{\partial \lambda} \tag{63}$$

The integration of the above differential equation is used to solve for $\bar{\delta}$ and λ using FORTRAN programming.

To start integration, initial values of $\bar{\delta}$ and λ are required as $\xi \to 0$. The asymptotic solution is given by:

$$\bar{\delta}_{1i} = C_1\bar{\delta}, \qquad \bar{\delta}_{2i} = C_2\bar{\delta} \tag{64}$$

where:

$$C_1 = -\left(\frac{a_{2,0}}{q+2} + \frac{a_{3,0}}{q+3}\right) \tag{65}$$

$$C_2 = -\left(\frac{a_{2,0}^2}{2q+3} + \frac{a_{3,0}^2}{2q+5} + \frac{a_{3,0}}{q+3} + \frac{a_{2,0}(a_{3,0}+1)}{q+2}\right) \tag{66}$$

Where subscript 0 refers to values of a_2 and a_3 at $\lambda = 0$.

Using equations (51) and (52) yields

$$\bar{\delta} = \left[\frac{(4\alpha_o)^n (n+1)\xi}{C_2}\right]^{\frac{1}{n+1}} \tag{67}$$

$$\lambda = \frac{C_1 \alpha_o \bar{\delta}}{C_2} \tag{68}$$

where

$$\alpha_o = q - a_2 - 2a_3 \tag{69}$$

Defining the ratio of the above with C_1 and C_2 gives C:

where,

$$C = \frac{\lambda}{\bar{\bar{\delta}}} \tag{70}$$

For n=1, we have $C_1 = 0.3, C_2 = 0.11746$ and $\alpha_o = 2$.

3.3. Filled Region

In the filled region, the boundary layer fills the entire core region of the cross section of the parallel plate channel.

Core region:

$$U_c \frac{dU_c}{dx} = -\frac{1}{\rho}\frac{\partial P}{\partial x} + \frac{K}{\rho}\frac{\partial}{\partial y}\left[\left(\frac{\partial u}{\partial y}\right)^n\right]_{y=a} \tag{71}$$

Boundary layer region:

$$u\frac{\partial u}{\partial x} + v\frac{\partial u}{\partial y} = \frac{K}{\rho}\frac{\partial}{\partial y}\left[\left(\frac{\partial u}{\partial y}\right)^n\right] + U_c\frac{dU_c}{dx} - \frac{K}{\rho}\frac{\partial}{\partial y}\left[\left(\frac{\partial u}{\partial y}\right)^n\right]_{y=a} \tag{72}$$

where, u and v are the velocity components in the x and y directions, respectively, ρ is the fluid density, U_c is the centreline velocity and P denotes the pressure.

Following Chebbi [25], we define $\alpha\ and\ \lambda$ in the filled region as,

$$\alpha = \frac{a}{U_c}\left(\frac{du}{dy}\right)_{y=0} \tag{73}$$

$$\lambda = \frac{\rho}{K}\frac{\delta^{n+1}}{\alpha^{n-1}}\frac{1}{U_c^{n-1}}\frac{dU_c}{dx} \tag{74}$$

The boundary conditions in the filled region are:

$$u = 0, v = 0 \qquad \text{at y} = 0 \tag{75}$$

$$u = U_c, \frac{\partial u}{\partial y} = 0, \qquad \text{at y} = \text{a} \tag{76}$$

where a denotes half of the channel width, and U_c is the centerline velocity.

The shape factor is defined in the filled region as:

$$\Gamma = \left(\frac{\partial u}{\partial y}\right)_{y=a}^{n-1} \left(\frac{\partial^2 u}{\partial y^2}\right)_{y=a} \frac{na^{n+1}}{\alpha^{n-1} U_c^n} \tag{77}$$

It is used to account for the deviation of the velocity profile from the fully developed one at the end of the entrance region.

The equation of continuity gives:

$$\frac{\partial u}{\partial x} = -\frac{\partial v}{\partial y} \tag{78}$$

Therefore,

$$u\frac{\partial u}{\partial x} = \frac{\partial u^2}{\partial x} - u\frac{\partial u}{\partial x} \tag{79}$$

Applying the equation of continuity (78) yields

$$u\frac{\partial u}{\partial x} = \frac{\partial u^2}{\partial x} + u\frac{\partial v}{\partial x} \tag{80}$$

Substituting this equation (80), in the boundary layer equation (72) provides

$$\frac{\partial u^2}{\partial x} + u\frac{\partial v}{\partial x} + v\frac{\partial u}{\partial y} = \frac{K}{\rho}\frac{\partial}{\partial y}\left[\left(\frac{\partial u}{\partial y}\right)^n\right] + U_c\frac{dU_c}{dx} - \frac{K}{\rho}\frac{\partial}{\partial y}\left[\left(\frac{\partial u}{\partial y}\right)^n\right]_{y=a} \tag{81}$$

Integrating the above equation with respect to y from $y = 0$ to $y = a$ yields

$$\begin{aligned}\int_0^a \frac{\partial u^2}{\partial x} dy + \int_0^a \frac{\partial (uv)}{\partial y} dy \\ = \int_0^a \frac{K}{\rho}\frac{\partial}{\partial y}\left[\left(\frac{\partial u}{\partial y}\right)^n\right] dy + \int_0^a U_c \frac{dU_c}{dx} dy \\ - \int_0^a \frac{K}{\rho}\frac{\partial}{\partial y}\left[\left(\frac{\partial u}{\partial y}\right)^n\right]_{y=a} dy\end{aligned} \tag{82}$$

Applying the boundary conditions, we obtain:

$$\frac{d}{dx}\int_0^a u^2\, dy = \frac{dU_c}{dx}\int_0^a U_c\, dy - \frac{K(a)}{\rho}\frac{\partial}{\partial y}\left[\left(\frac{\partial u}{\partial y}\right)^n\right]_{y=a} - \frac{K}{\rho}\left[\left(\frac{\partial u}{\partial y}\right)^n\right]_{y=0} \tag{83}$$

Subtracting $\frac{d}{dx}\int_0^a uU_c\,dy$ from both sides of equation (83) we get:

$$\frac{d}{dx}\int_0^a (u^2 - uU_c)\,dy + \int_0^a U_c \frac{\partial u}{\partial x} dy + \frac{dU_c}{dx}\int_0^a u\,dy = \frac{dU_c}{dx}\int_0^a U_c\,dy - \frac{K(a)}{\rho}\frac{\partial}{\partial y}\left[\left(\frac{\partial u}{\partial y}\right)^n\right]_{y=a} - \frac{K}{\rho}\left[\left(\frac{\partial u}{\partial y}\right)^n\right]_{y=0} \tag{84}$$

The equation of continuity yields:

$$\int_0^a \frac{\partial u}{\partial x} dy = 0 \tag{85}$$

Applying the above equation (85) in equation (84):

$$\frac{d}{dx}\left[U_c^2\int_0^a \frac{u}{U_c}\left(1-\frac{u}{U_c}\right)dy\right] + U_c\frac{dU_c}{dx}\int_0^a \left(1-\frac{u}{U_c}\right)dy = \frac{K(a)}{\rho}\frac{\partial}{\partial y}\left[\left(\frac{\partial u}{\partial y}\right)^n\right]_{y=a} + \frac{K}{\rho}\left[\left(\frac{\partial u}{\partial y}\right)^n\right]_{y=0} \tag{86}$$

We define the displacement thickness, δ_{1f} and momentum thickness, δ_{2f} in the filled region as:

$$\delta_{2f} = \int_0^a \frac{u}{U_c}\left[1-\frac{u}{U_c}\right]dy \tag{87}$$

$$\delta_{1f} = \int_0^a \left[1-\frac{u}{U_c}\right]dy \tag{88}$$

Substituting the above definitions in equation (86), we get:

$$U_c^2\frac{d\delta_{2f}}{dx} + U_c\frac{dU_c}{dx}\left[2\delta_{2f} + \delta_{1f}\right] = \frac{K(a)}{\rho}\frac{\partial}{\partial y}\left[\left(\frac{\partial u}{\partial y}\right)^n\right]_{y=a} + \frac{K}{\rho}\left[\left(\frac{\partial u}{\partial y}\right)^n\right]_{y=0} \tag{89}$$

3.3.1. Conservation of mass in the filled region

The overall mass balance is as followed:

$$\int \rho u dA = \rho U_o A \tag{90}$$

Dividing by $2w\rho$ on both sides:

$$aU_o = \int_0^a u\,dy \tag{91}$$

Then, dividing by U_c on both sides to the above equation:

$$\frac{aU_o}{U_c} = \int_0^a \frac{u}{U_c} dy \tag{92}$$

Integrating with respect to y gives:

$$\frac{aU_o}{U_c} = \int_0^a \frac{u}{U_c} dy \tag{93}$$

Rearranging the above equation gives:

$$\int_0^a \left(1 - \frac{u}{U_c}\right) dy = a\left(1 - \frac{U_o}{U_c}\right) \tag{94}$$

Equation (94), yields:

$$\delta_{1f} = a\left(1 - \frac{U_o}{U_c}\right) \tag{95}$$

Hence, the conservation of mass in the filled region gives:

$$\frac{U_o}{U_c} = 1 - \frac{\delta_{1f}}{a} \tag{96}$$

3.3.2. Dimensionless form in the filled region

Defining the dimensionless displacement thickness, momentum thickness and the centreline velocity below:

$$\bar{\delta}_{1f} = \frac{\delta_{1f}}{a} \tag{97}$$

$$\bar{\delta}_{2f} = \frac{\delta_{2f}}{a} \tag{98}$$

$$\overline{U}_c = \frac{U_c}{U_o} \tag{99}$$

The dimensionless coordinate in the y-direction is defined as:

$$\zeta = 1 - \frac{y}{a} \tag{100}$$

Also, the dimensionless local friction factor is expressed as followed:

$$C_f\,Re = 2\left\lfloor 4^n \alpha^n \overline{U}_c{}^n \right\rfloor \tag{101}$$

The dimensionless equation of conservation of mass in the filled region is obtained from equation (96)

$$\frac{1}{\overline{U}_c} = 1 - \bar{\delta}_{1f} \tag{102}$$

The dimensionless form of equation (88) is shown below:

$$\overline{U}_c{}^2 \frac{d\bar{\delta}_{2f}}{d\xi} + \overline{U}_c \frac{d\overline{U}_c}{d\xi}\left[2\bar{\delta}_{2f} + \bar{\delta}_{1f}\right] = -4^n \overline{U}_c{}^n \left[\frac{\partial}{\partial \zeta}\left(-\frac{\partial \bar{u}}{\partial \zeta}\right)^n_{\zeta=0} - \left(-\frac{\partial \bar{u}}{\partial \zeta}\right)^n_{\zeta=1}\right] \tag{103}$$

The rate of change of dimensionless displacement $\bar{\delta}_{1f}$ and momentum $\bar{\delta}_{2f}$ thickness with respect to ξ are given by:

$$\frac{d\bar{\delta}_{1f}}{d\xi} = \lambda\, 4^n \overline{U}_c{}^{n-3} \alpha^{n-1} \tag{104}$$

$$\frac{d\bar{\delta}_{2f}}{d\xi} = 4^n \overline{U}_c{}^{n-2} \alpha^{n-1}\left[\Gamma + \alpha - \lambda\left(2\bar{\delta}_{2f} + \bar{\delta}_{1f}\right)\right] \tag{105}$$

3.3.3. Solution of the filled region flow problem

To solve the above equations, the dimensionless velocity profile (53) is used. Using the boundary conditions gives:

Using the boundary conditions in equation (53) the filled region gives:

$$(a_1 + a_2 + a_3) = -1 \tag{106}$$

where,

$$a_1 = -\frac{(-\Gamma)^{\frac{1}{n}} \alpha^{\frac{n-1}{n}}}{q} \tag{107}$$

$$a_2 = \left[-1 + \frac{(-\Gamma)^{\frac{1}{n}} \alpha^{\frac{n-1}{n}}}{q}\right] - \frac{\frac{\Gamma - \lambda}{n} + \frac{q}{n} - 2q\left[-1 + \frac{(-\Gamma)^{\frac{1}{n}} \alpha^{\frac{n-1}{n}}}{q}\right]}{2q + 2} \tag{108}$$

$$a_3 = \frac{\frac{\Gamma - \lambda}{n} + \frac{q}{n} - 2q\left[-1 + \frac{(-\Gamma)^{\frac{1}{n}}\alpha^{\frac{n-1}{n}}}{q}\right]}{2q+2} \tag{109}$$

Thus, the approximate velocity profile in the filled region is given by:

$$\begin{aligned} \bar{u} = (1+\zeta^q)\Bigg(& -\frac{(-\Gamma)^{\frac{1}{n}}\alpha^{\frac{n-1}{n}}}{q} \\ & + \left\{\left[-1 + \frac{(-\Gamma)^{\frac{1}{n}}\alpha^{\frac{n-1}{n}}}{q}\right] - \frac{\frac{\Gamma - \lambda}{n} + \frac{q}{n} - 2q\left[-1 + \frac{(-\Gamma)^{\frac{1}{n}}\alpha^{\frac{n-1}{n}}}{q}\right]}{2q+2}\right\}\zeta \\ & + \left\{\frac{\frac{\Gamma - \lambda}{n} + \frac{q}{n} - 2q\left[-1 + \frac{(-\Gamma)^{\frac{1}{n}}\alpha^{\frac{n-1}{n}}}{q}\right]}{2q+2}\right\}\zeta^2\Bigg) \end{aligned} \tag{110}$$

Using velocity profile, the displacement thickness, $\bar{\delta}_{1f}$ is found by integration:

$$\bar{\delta}_{1f} = -\left(\frac{a_1}{q+1} + \frac{a_2}{q+2} + \frac{a_3}{q+3}\right) \tag{111}$$

Similarly, the momentum thickness, $\bar{\delta}_{2f}$ is obtained by integration using MATLAB:

$$\begin{aligned} \bar{\delta}_{2f} = -\Bigg(& \frac{a_2^2 + 2a_1a_3}{2q+3} + \frac{a_1^2}{2q+1} + \frac{a_3^2}{2q+5} + \frac{a_3}{q+3} + \frac{a_1(a_2+1)}{q+1} \\ & + \frac{a_2(a_3+1)}{q+2}\Bigg) \end{aligned} \tag{112}$$

The rates of change of dimensionless displacement $\bar{\delta}_{1f}$ and momentum $\bar{\delta}_{2f}$thickness with respect to ξ are obtained using the chain rule:

$$\frac{d\Gamma}{d\xi} = \frac{\frac{d\bar{\delta}_{1f}}{d\xi} G_{22f} - \frac{d\bar{\delta}_{2f}}{d\xi} G_{12f}}{G_{11f} G_{22f} - G_{21f} G_{12f}} \tag{113}$$

$$\frac{d\lambda}{d\xi} = \frac{\frac{d\bar{\delta}_{2f}}{d\xi} G_{11f} - \frac{d\bar{\delta}_{1f}}{d\xi} G_{21f}}{G_{11f} G_{22f} - G_{21f} G_{12f}} \tag{114}$$

where,

$$G_{11i} = \frac{\partial \bar{\delta}_{1f}}{\partial \Gamma}, \qquad G_{12i} = \frac{\partial \bar{\delta}_{1f}}{\partial \lambda}, \qquad G_{21i} = \frac{\partial \bar{\delta}_{2f}}{\partial \Gamma}, \qquad G_{22i} = \frac{\partial \bar{\delta}_{2f}}{\partial \lambda} \tag{115}$$

The integration of the above differential equation is used to solve for λ and Γ in the filled region using FORTRAN programming.

To start this integration, initial values of Γ and λ are required. The initial value of Γ is taken as 0. The value of λ at the end of the inlet region is used as the starting value in the filled region. The pressure drop is obtained by integrating the following using equation (71):

$$\frac{d\Delta\bar{P}}{d\xi} = 2\bar{U}_c \frac{d\bar{U}_c}{d\xi} - 2(4^n)\bar{U}_c^{\ n} \Gamma \alpha^{n-1} \tag{116}$$

The rate of change of $\bar{U}_c$ with respect to ξ is determined using equation (74) as:

$$\frac{d\bar{U}_c}{d\xi} = \lambda \alpha^{n-1} \bar{U}_c^{\ n-1} 4^{\mathrm{n}} \tag{117}$$

3.4. Fully-Developed Flow

The entrance region includes both the inlet and filled regions. The fully developed velocity is given in Bird et al. [27] below:

$$u = \left(\frac{(P_O - P)\, a}{KL}\right)^{\frac{1}{n}} \frac{a}{\left(\frac{1}{n} + 1\right)} \left[1 - \left(\frac{y}{a}\right)^{\frac{1}{n}+1}\right] \qquad 0 \le y \le a \tag{118}$$

The dimensionless velocity profile in the fully developed region is given by:

$$\bar{u}_{fd} = 1 - \zeta^q \tag{119}$$

Differentiating the above expression with respect to ξ yields:

$$\frac{d\bar{u}_{fd}}{d\xi} = -q\zeta^{q-1} \tag{120}$$

Differentiating the above for the second derivative with respect to ξ gives:

$$\frac{d^2\bar{u}_{fd}}{d\xi^2} = -q(q-1)\zeta^{q-2} \tag{121}$$

The fully developed value, λ_{fd} is zero:

$$\lambda_{fd} = 0 \tag{122}$$

The value of α_{fd} is given by:

$$\alpha_{fd} = \left(-\frac{d\bar{u}_{fd}}{d\xi}\right)_{\zeta=1} = q \tag{123}$$

Substituting the above equations in equations (76) and equation (101) gives the fully developed values, Γ_{fd} and $C_{f,fd}\,Re$:

$$\Gamma_{fd} = -q \tag{124}$$

$$C_{f,fd}\,Re = 2(4^n)\left[q\bar{U}_{c_{fd}}\right]^n \tag{125}$$

where the centreline velocity, $\overline{U}_{c_{fd}}$ is given by:

$$\bar{U}_{c_{fd}} = \frac{2n+1}{n+1} \tag{126}$$

Using the above equations, the entrance region problem is solved by solving for $\bar{\delta}$, λ and Γ versus the dimensionless axial distance. $\bar{\delta}$ and λ are found by integrating equations (61) and (62) with Γ is equal to 0 in the inlet region. The filled region begins at the end of the inlet region where $\bar{\delta}$ reaches a value of one.

In the filled region, Γ and λ are found by integrating equations (113) and (114). Moreover, using equations (47), (48) and (49), pressure drop, the local friction factor, and the centreline velocity are obtained in the inlet region, and using equations (100),

$$\alpha = 1 + a_1 - a_3 + q \tag{127}$$

(101) and (102) in the filled region, where α is given by:

Figures 4-1, 4-2, 4-3, 4-4, 4-5 and 4-6 illustrate the profiles for various values of n ($n = 0.75,\ 1, 1.5$ and 2) for $\bar{\delta}$, λ, Γ, the local friction factor, pressure-drop, and the centerline velocity respectively. These profiles are compared with the results of Al Ali [28] and are found in good agreement with the present results for the case of Newtonian fluid, n equal to 1. The dimensionless boundary layer thickness profile in Figure 4-1 is also compared with Crespí-Llorens and Galanis [19] and Mohanty and Das [23] for the case of Newtonian fluid. The present boundary layer thickness results for the Newtonian fluid case coincide perfectly with both Al Ali [28] and Mohanty and Das [23] results. The results of Crespí-Llorens and Galanis [19] show deviations.

The pressure-drop profile in Figure 4-5 is compared with Goldstein [21] and Bodoia and Osterle [16] results for Newtonian fluid and demonstrates strong consistency. The centerline velocity profiles shown in Figure 4-6 show good agreement with both Al Ali [28] and Bodoia and Osterle [16] results for Newtonian fluid whereas Crespí-Llorens and Galanis [19] results for $n = 0.75$ and $n = 1$ exhibit discrepancy from the present results knowing that Bodoia and Osterle [16] results are considered as the most accurate by Shah and Bhati [29], as mentioned by Crespi-Llorens and Galanis [19]. Figure 4-7 depicts the entrance region length which is defined as the location where the centerline velocity reaches 99% of its fully developed value.

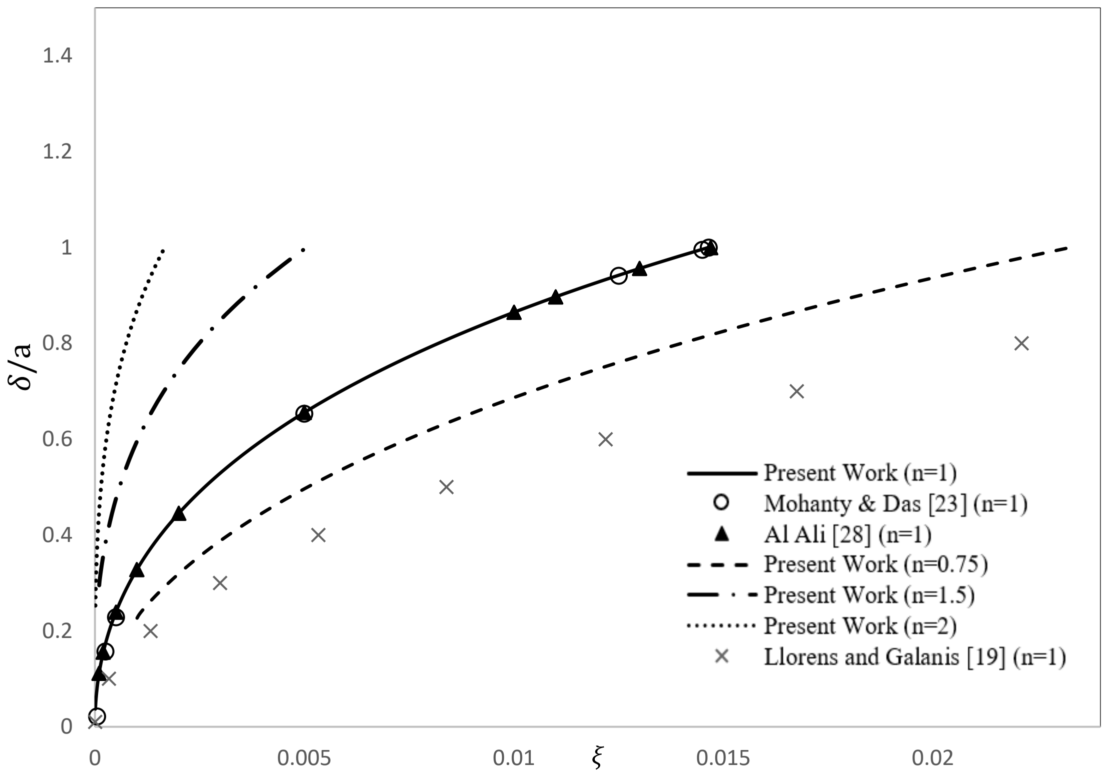

Figure 4-1: Dimensionless boundary layer thickness profiles.

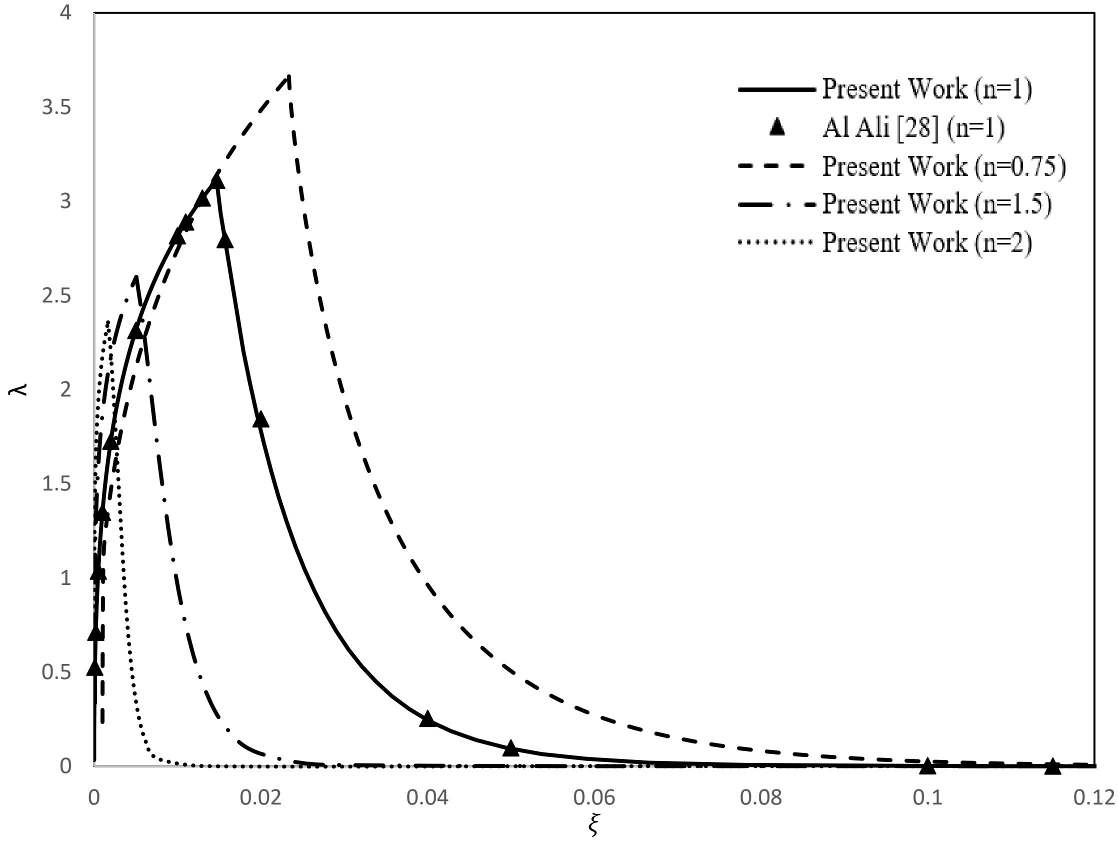

Figure 4-2: Profiles for λ.

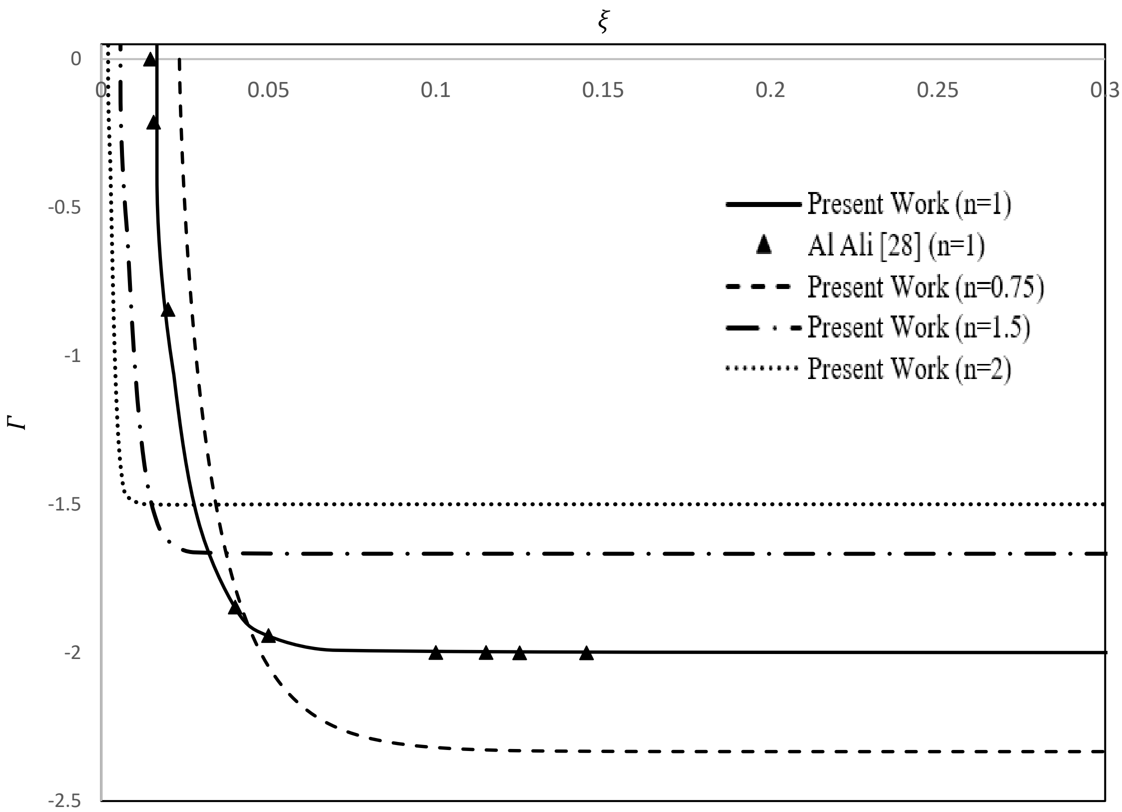

Figure 4-3: Profiles for Γ.

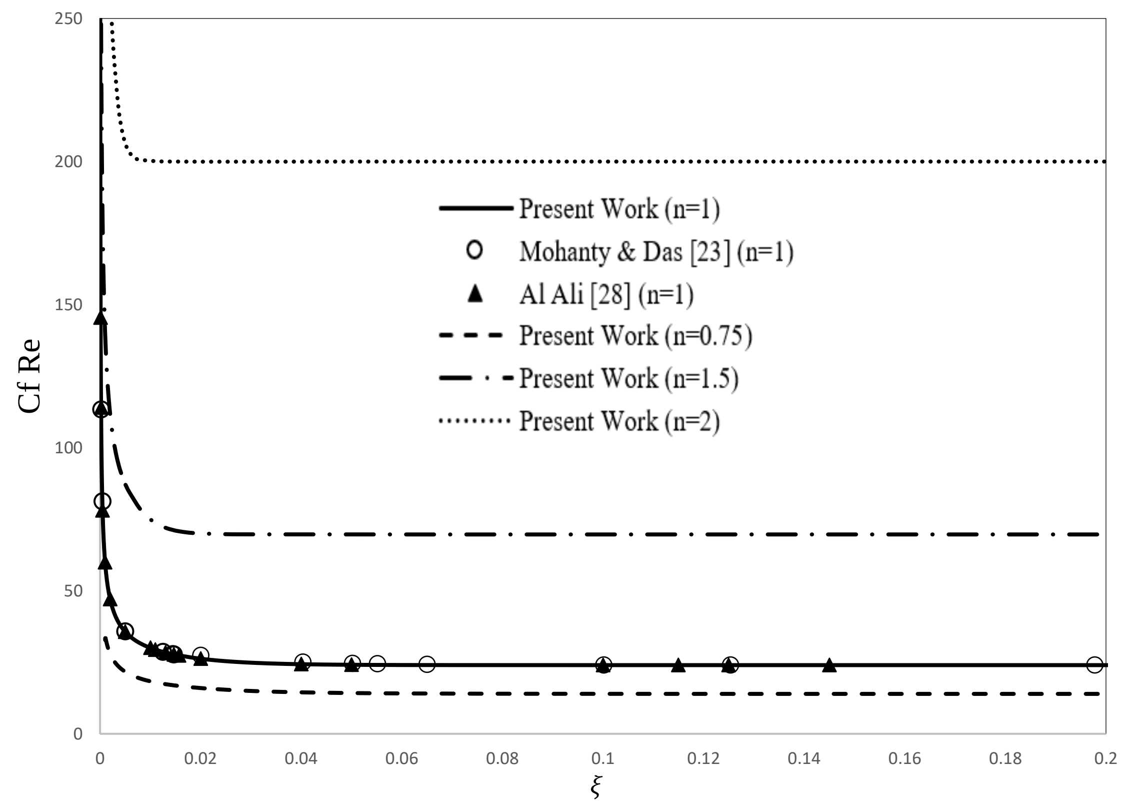

Figure 4-4: Local friction factor profiles.

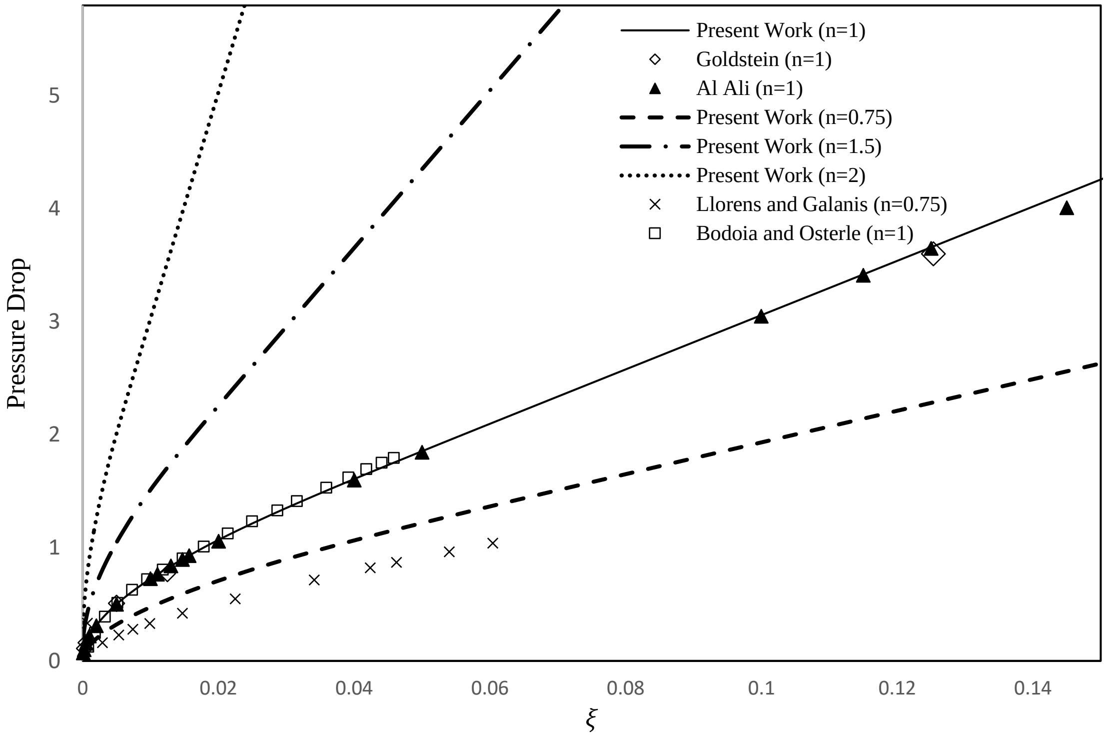

Figure 4-5: Pressure drop profiles.

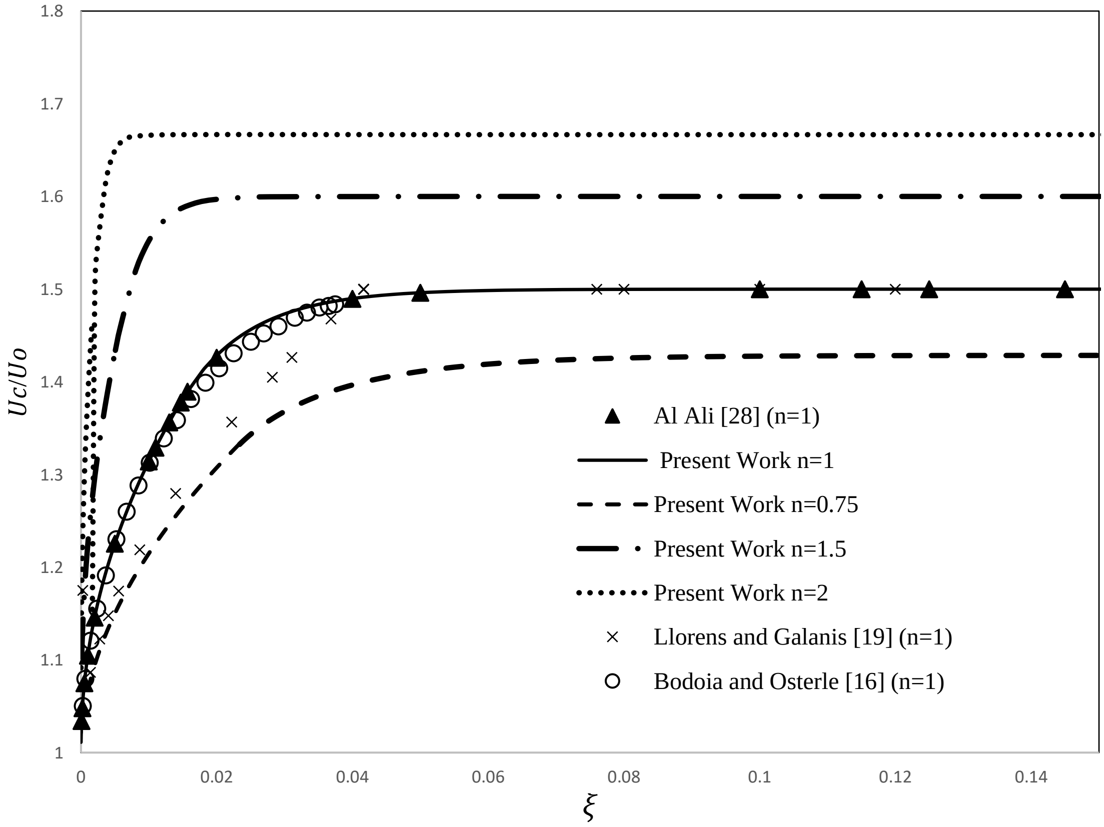

Figure 4-6: Centreline velocity profiles.

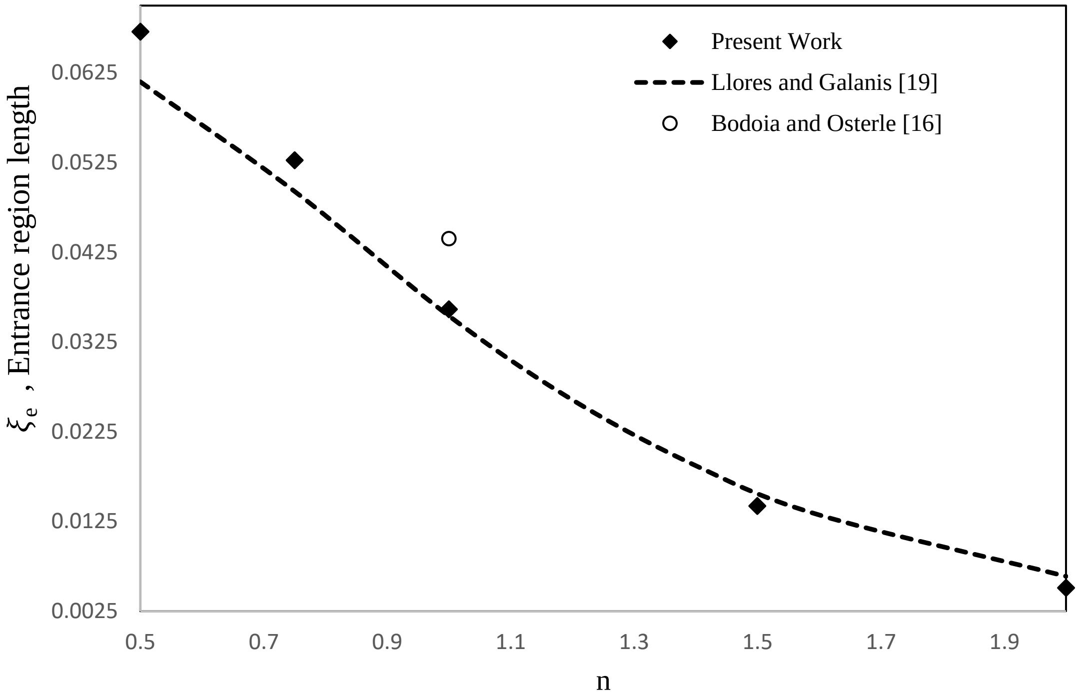

Figure 4-7: Entrance region length versus n.

Chapter 5. Conclusion and Future Work

5.1. Summary

Chapter 1 introduces non-Newtonian fluid flow between parallel plates and the inlet-filled region concept. As reported by Lambride et al. [20], entry length determination has several major applications including hemodynamics [30], microfluidics [31], rheometry [32] and piping systems design including transition to turbulence [33]. Chapter 2 explains the boundary layer theory and earlier work done by numerous researchers to solve this problem. Chapter 3 provides the inlet-filled region model used to solve the problem by extending the method of Mohanty and Das [23] to power-law fluid flow between two parallel plates using a velocity profile matching asymptotically the fully developed velocity profile. Chapter 4 discusses the results and compares them with the literature [16, 19, 21, 28].

5.2. Conclusion

In this study, the laminar flow with constant wall temperature of a non-Newtonian power-law fluid between parallel plates was investigated using the inlet-filled concept and modified boundary layer integral method. The results for both the inlet and filled regions include the profiles for the entrance region length, boundary layer thickness, pressure-drop, the local friction factor, and the centreline velocity for the different values of the power-law fluid index, n. The present results are in good agreement with the results of Al Ali [28], Goldstein [21] and, Bodoia and Osterle [16].

5.3. Future Work

As a prospective investigation, experimental work for various values of n should be studied to further compare the boundary layer thickness, pressure-drop, the local friction factor, and the centreline velocity profiles presented in this thesis.

References

[1] A. Lenci and L. Chiapponi, “An experimental setup to investigate non-Newtonian fluid flow in variable aperture channels,” *Water,* vol. 12, no. 5, p. 1284, May 2020, doi: 10.3390/w12051284.

[2] P. Saramito, *Complex fluids: Modeling and Algorithms*. Springer, 2016.

[3] S. Ishizawa, “The axi-symmetric laminar flow in an arbitrarily shaped narrow gap: (2nd Report, Theoretical Analysis for the Downstream Region),” *Bulletin of the JSME*, vol. 9, no. 33, pp. 86–103, Jan. 1966, doi: 10.1299/jsme1958.9.86.

[4] Y. J. Xu, M. Bilal, Q. Al-Mdallal, M. A. Khan, and T. Muhammad, “Gyrotactic micro-organism flow of Maxwell nanofluid between two parallel plates,” *Sci Rep*, vol. 11, no. 1, Dec. 2021, doi: 10.1038/s41598-021-94543-4.

[5] Z. Huang, B. Li, X. Si, and C. Yao, “Natural convection and radiation heat transfer of power-law fluid food in symmetrical open containers,” *J Therm Anal Calorim,* vol. 144, no. 4, pp. 1287–1298, May 2021, doi: 10.1007/s10973-020-09616-9.

[6] A. Tanveer, T. Salahuddin, M. Khan, M. Y. Malik, and M. S. Alqarni, “Theoretical analysis of non-Newtonian blood flow in a microchannel,” *Comput Methods Programs Biomed*, vol. 191, Jul. 2020, doi: 10.1016/j.cmpb.2019.105280.

[7] A. K. Mohanty and S. B. L. Asthana, “Laminar flow in the entrance region of a smooth pipe,” *Journal of Fluid Mechanics,* vol. 90, no. 3, pp. 433–447, Feb. 1979, doi: 10.1017/s0022112079002330

[8] N. De Nevers, *Fluid mechanics for chemical engineers,* 3rd ed. [Illustrated]. New York, NY: McGraw-Hill Higher Education, 2005.

[9] Tani, “History of Boundary Layer Theory,” *Annual Review of Fluid Mechanics*, vol. 9, no. 1, pp. 87–111, Jan. 1977, doi: 10.1146/annurev.fl.09.010177.000511.

[10] L. Schiller, “Die Entwicklung der laminaren Geschwindigkeitsverteilung und ihre Bedeutung für Zähigkeitsmessungen., (Mit einem Anhang über den Druckverlust turbulenter Strömung beim Eintritt in ein Rohr.),” *Journal of Applied Mathematics and Mechanics*, vol. 2, no. 2, pp. 96–106, Jan. 1922, doi: 10.1002/zamm.19220020203.

[11] H. L. Langhaar, “Steady flow in the transition length of a straight tube,” *Journal of Applied Mechanics*, vol. 9, no. 2, pp. A55–A58, Jun. 1942, doi: 10.1115/1.4009183.

[12] J. Boussinesq, *Notice sur les travaux scientifiques de M. J. Boussinesq*. L. Danel, 1883. Available: https://books.google.ae/books/about/Notice_sur_les_travaux_scientifiques_de.html?id=SPu-A0JmLzcC&redir_esc=y

[13] S. Goldstein, *Modern Developments in Fluid Dynamics: An Account of Theory and Experiment Relating to Boundary Layers, Turbulent Motion and Wakes*. Clarendon Press, 1950.

[14] R. J. Siegel and A. H. Shapiro, "The effect of heating on boundary layer transition for liquid flow in a tube," 1953. [Online]. Available: https://dspace.mit.edu/handle/1721.1/36438

[15] W. B. Campbell and J. T. Slattery, "Flow in the entrance of a tube," *Journal of Basic Engineering*, vol. 85, no. 1, pp. 41–45, Mar. 1963, doi: 10.1115/1.3656529.

[16] J. R. Bodoia and J. F. Osterle, "Finite difference analysis of plane Poiseuille and Couette flow developments," *Applied Scientific Research*, vol. 10, no. 1, pp. 265–276, Jan. 1961, doi: 10.1007/bf00411919.

[17] S.-W. Yau and C. Tien, "Simultaneous development of velocity and temperature profiles for laminar flow of a non-Newtonian fluid in the entrance region of flat ducts," *Canadian Journal of Chemical Engineering*, vol. 41, no. 4, pp. 139–145, Aug. 1963, doi: 10.1002/cjce.5450410402.

[18] R. N. O. Magno, E. N. Macêdo, and J. N. N. Quaresma, "Solutions for the internal boundary layer equations in simultaneously developing flow of power-law fluids within parallel plates channels," *Chemical Engineering Journal*, vol. 87, no. 3, pp. 339–350, Aug. 2002, doi: 10.1016/s1385-8947(01)00302-3.

[19] D. Crespí-Llorens and N. Galanis, "Laminar forced convection of power-law fluids in the entrance region of parallel plates ducts," *International Journal of Heat and Mass Transfer*, vol. 115, pp. 991–1003, Dec. 2017, doi: 10.1016/j.ijheatmasstransfer.2017.08.093.

[20] C. Lambride, A. Syrakos, and G. C. Georgiou, "Entrance length estimates for flows of power-law fluids in pipes and channels," *Journal of Non-newtonian Fluid Mechanics*, vol. 317, Art. no. 105056, Apr. 2023, doi: 10.1016/j.jnnfm.2023.105056.

[21] L. M. Milne-Thomson and S. Goldstein, "Modern developments in fluid dynamics," *The Mathematical Gazette*, vol. 23, no. 254, p. 219, May 1939, doi: 10.2307/3607555.

[22] L. Rosenhead and L. Talbot, "Laminar boundary layers," *Physics Today*, vol. 17, no. 6, pp. 62–63, Jun. 1964, doi: 10.1063/1.3051660.

[23] A. K. Mohanty and R. Das, "Laminar flow in the entrance region of a parallel plate channel," *AIChE Journal*, vol. 28, no. 5, pp. 830–833, Sep. 1982, doi: 10.1002/aic.690280520.

[24] H. H. Al-Ali and M. S. Selim, "Simultaneous development of velocity and temperature profiles in the entrance region of a parallel plate channel: laminar flow with uniform wall heat flux," *Chemical Engineering Communications*, vol. 112, no. 1, pp. 1–19, Feb. 1992, doi: 10.1080/00986449208935988.

[25] R. Chebbi, “Laminar flow of power-law fluids in the entrance region of a pipe,” *Chemical Engineering Science*, vol. 57, no. 21, pp. 4435–4443, Nov. 2002, doi: 10.1016/s0009-2509(02)00422-0.

[26] B. Baioumy, R. Chebbi, and N. A. Jabbar, “Bingham fluid flow in the entrance region of a pipe,” *Journal of Fluids Engineering-transactions of the Asme*, vol. 143, no. 2, Feb. 2021, doi: 10.1115/1.4048610.

[27] R. B. Bird, W. E. Stewart, and E. N. Lightfoot, *Transport Phenomena*. John Wiley & Sons, 2006.

[28] H. H. Al-Ali, “Simultaneously developing laminar flow and heat transfer in the entrance region of flat and circular conduits,” Colorado School of Mines, 1988. Accessed: Apr. 01, 2024. Available: https://repository.mines.edu/handle/11124/177055

[29] R. K. Shah and M. S. Bhatti, "Laminar convective heat transfer in ducts," in Handbook of single-phase convective heat transfer, New York: John Wiley, 1987.

[30] J.B. Grotberg, "Biofluid Mechanics: Analysis and Applications," Cambridge University Press, Cambridge, 2021.

[31] M.W. Lee, K.H. Yu, Y.H. Teoh, H.W. Lee, and M.A. Ismail, "Developing flow of power law fluids in circular tube having superhydrophobic transverse grooves," J. Adv. Res. Fluid Mech. Thermal Sci., vol. 56, pp. 1–9, 2019.

[32] C. Fernandes, L. J. L. Ferrás, M. S. B. Araújo, and J. M. Nóbrega, “Development length in planar channel flows of inelastic non-Newtonian fluids,” Journal of non-Newtonian Fluid Mechanics, vol. 255, pp. 13–18, May 2018, doi: 10.1016/j.jnnfm.2018.02.011.

[33] R.J. Poole and S.B. Ridley, "Development length requirements for fully-developed laminar pipe flow of inelastic non-Newtonian liquids," ASME J. Fluids Eng., vol. 129, pp. 1281–1287, 2007.

Vita

Sadia Rehman was born and raised in Ras Al Khaimah, United Arab Emirates. She received her primary and secondary education in Ras Al Khaimah, UAE and received her B.Sc. degree in Chemical Engineering from the American University of Ras Al Khaimah in January 2022. She worked as a R&D Engineer at Tenka Solar, Dubai from March to August 2022.

In September 2022, she joined the Chemical Engineering master's program in the American University of Sharjah as a graduate teaching assistant.